

OPEN

# Production of reactive species in alginate hydrogels for cold atmospheric plasma-based therapies

Cédric Labay<sup>1,2,3</sup>, Inès Hamouda<sup>1,2,3</sup>, Francesco Tampieri<sup>1,2,3</sup> , Maria-Pau Ginebra<sup>1,2,3,4</sup> & Cristina Canal<sup>1,2,3\*</sup> 

In the last years, great advances have been made in therapies based in cold atmospheric plasmas (CAP). CAP generate reactive oxygen and nitrogen species (RONS) which can be transferred to liquids. These CAP activated liquids display the same biological efficacy (i.e. on killing cancer cells) as CAP themselves, opening the door for minimally invasive therapies. However, injection of a liquid in the body results in fast diffusion due to extracellular fluids and blood flow. Therefore, the development of efficient vehicles which allow local confinement and delivery of RONS to the diseased site is a fundamental requirement. In this work, we investigate the generation of RONS ( $\text{H}_2\text{O}_2$ ,  $\text{NO}_2^-$ , short-lived RONS) in alginate hydrogels by comparing two atmospheric pressure plasma jets: kINPen and a helium needle, at a range of plasma treatment conditions (time, gas flow, distance to the sample). The physico-chemical properties of the hydrogels remain unchanged by the plasma treatment, while the hydrogel shows several-fold larger capacity for generation of RONS than a typical isotonic saline solution. Part of the RONS are quickly released to a receptor media, so special attention has to be put on the design of hydrogels with *in-situ* crosslinking. Remarkably, the hydrogels show capacity for sustained release of the RONS. The plasma-treated hydrogels remain fully biocompatible (due the fact that the species generated by plasma are previously washed away), indicating that no cytotoxic modifications have occurred on the polymer. Moreover, the RONS generated in alginate solutions showed cytotoxic potential towards bone cancer cells. These results open the door for the use of hydrogel-based biomaterials in CAP-associated therapies.

Plasma is defined as a totally or partially ionized gas that contains a high number of reactive species, ions, electrons, metastable particles, etc. The development of plasma sources of small dimensions and able to operate at atmospheric pressure and at temperatures close to room temperature has fostered the development of a new field named Plasma medicine<sup>1</sup>. Atmospheric pressure plasma (APP) has been evaluated as an effective tool for sterilization<sup>2</sup>, cancer treatment<sup>3</sup> or for enhancing wound healing<sup>4</sup>. APPs formed in air generate reactive oxygen and nitrogen species (RONS), which can be transferred to liquids through secondary reactions. Plasma-activated liquids (PAL) display different biological actions which have been mainly attributed to the generation of RONS such as hydrogen peroxides ( $\text{H}_2\text{O}_2$ ), nitrites ( $\text{NO}_2^-$ ), peroxy nitrites, etc. These reactive species are known to be involved in a wide range of intracellular and intercellular processes<sup>5</sup>. Until now, major attention has been paid in plasma medicine to the monitoring of RONS induced in PAL used in indirect treatments<sup>6</sup>, and some works have investigated their storage by freezing the PAL but this is not always possible<sup>7</sup>. However, transportation and diffusion from suitable biomaterials of these RONS for *in situ* therapy remains to be explored.

Hydrogels can be an asset for that aim, as they have characteristics such as biocompatibility, *in vivo* biodegradability and ductility that are key features in the design of advanced biomaterials<sup>8,9</sup>. These highly swollen 3D networks of macromolecules have emerged as powerful candidate biomaterials for the local delivery of a variety

<sup>1</sup>Biomaterials, Biomechanics and Tissue Engineering Group, Dpt. Materials Science and Metallurgy, Universitat Politècnica de Catalunya (UPC), Escola d'Enginyeria Barcelona Est (EEBE), c/Eduard Maristany 14, 08019, Barcelona, Spain. <sup>2</sup>Barcelona Research Center in Multiscale Science and Engineering, UPC, Barcelona, Spain. <sup>3</sup>Research Centre for Biomedical Engineering (CREB), UPC, Barcelona, Spain. <sup>4</sup>Institute for Bioengineering of Catalonia (IBEC), Barcelona Institute of Science and Technology (BIST), c/Baldiri i Reixach 10-12, 08028, Barcelona, Spain. \*email: [cristina.canal@upc.edu](mailto:cristina.canal@upc.edu)

of drugs at physiologically relevant doses for prolonged periods of time. Our hypothesis is that due to their high water contents and porous network they could be suitably used as carrier for RONS generated in plasma-activated liquid, providing new alternatives for therapies based on cold plasmas. Hydrogels can be based on natural polymers (e.g. polysaccharides, gelatine and fibrin), synthetic polymers (e.g. ethylene oxide, vinyl alcohol or acrylic acid) or semi-synthetic polymers (mixture between both natural and synthetic polymers)<sup>10</sup>. Hydrogels obtained from natural polymers have many advantages including low toxicity and good biocompatibility<sup>11</sup>. Alginate used in this work is obtained from brown algae and is typically used to produce hydrogels for a variety of applications in drug delivery and tissue engineering<sup>12</sup>. Alginate hydrogels can be prepared by simple gelation with divalent cations such as  $\text{Ca}^{2+}$ <sup>13,14</sup> so can be easily formed *in situ* in the body in contact with body fluids or in the lab in contact with  $\text{Ca}^{2+}$  containing solutions.

The purpose of this work is to evaluate the potential of employing alginate-based hydrogels as vehicles of RONS generated by atmospheric plasmas. Specifically, we analyse whether there are any chemical modifications in the structure of the alginate and its hydrogel-forming ability. In view of their possible therapeutic applications, their biological properties are investigated: biocompatibility of the plasma-treated polymer and cytotoxicity of the RONS generated therein.

## Results

**CAP produces high amount of RONS in alginate.** CAP treatments of several concentrations of alginate (between 0.2% and 2%) produced nitrites ( $\text{NO}_2^-$ ) and hydrogen peroxides ( $\text{H}_2\text{O}_2$ ) in all cases. However, plasma treatment of high concentrations of alginate revealed a hampered diffusion of the reactive species (Supplementary Fig. 1). Since this lack of homogeneity in the diffusion of the reagent influenced the precise detection of RONS, the solution of 0.5 wt% alginate was selected for further work.

Figure 1 presents the quantification of nitrites, hydrogen peroxide and short-lived species generated by plasma as a function of gas flow and distance to the sample in 0.5 wt% alginate or Ringer's saline, used as control, for 90 s plasma treatment time.

Plasma treatment of alginate allowed much higher generation of RONS ( $\text{NO}_2^-$ ,  $\text{H}_2\text{O}_2$  and short-lived species) than those obtained in Ringer's saline. In particular, the amounts of  $\text{NO}_2^-$  generated by APPJ in Ringer at gas flows above 2 L/min are very low and barely visible (Fig. 1(a) (ii)). For both kINPen and APPJ-treated alginate, a higher loading of  $\text{NO}_2^-$  was achieved for short distance to the sample and low gas flows (Fig. 1a). Higher concentrations of nitrites were generated using kINPen for all studied conditions.

The effects of plasma jet distance and gas flow on alginate followed a different trend when  $\text{H}_2\text{O}_2$  was concerned (Fig. 1b). Increasing gas flow rates led to higher concentration of  $\text{H}_2\text{O}_2$  in alginate, and short distances were still more suitable to generate higher amount of species. The amount of peroxides generated in Ringer's was several-fold lower than in alginate, and the effects of gas flow or distance were minimized. kINPen at 10 mm distance reached the highest concentrations of  $\text{H}_2\text{O}_2$ , but longer distances produced less peroxides than APPJ. Regarding APPJ, similar  $\text{H}_2\text{O}_2$  concentrations were obtained between 2 and 5 L/min disregard the distance between the liquid and the jet. The maximum amount of  $\text{H}_2\text{O}_2$  in alginate generated by APPJ was obtained using 15 mm nozzle distance and gas flow between 2 and 4 L/min.

kINPen treatment of 0.5% alginate and Ringer's saline highlighted that short distance enhances the generation of short-lived species (Fig. 1c). However, no significant differences were observed with the variation of gas flow for the alginate. The most efficient treatment of alginate with regard to the production of short-lived species was with kINPen at 10 mm distance and 1 L/min.

These results with plasma-treated alginate contrast with those obtained for plasma-activated Ringer's solution in which APPJ treatment was more effective than kINPen in similar conditions. As observed with the long-lived species recorded ( $\text{NO}_2^-$  and  $\text{H}_2\text{O}_2$ ), the capacity for generating RONS was much higher in alginate than in plasma-activated Ringer's saline, i.e. with up to 25 times higher concentrations of short-lived species for kINPen treatment of alginate with respect to physiological solution.

Plasma treatment time progressively increased the concentration of RONS ( $[\text{NO}_2^-]$ ,  $[\text{H}_2\text{O}_2]$  and short-lived species) in 0.5% alginate with both plasma jets (Fig. 2a). While the generation of  $\text{H}_2\text{O}_2$  was relatively similar between kINPen and APPJ, it was observed that, independently of plasma treatment time, kINPen generated more  $\text{NO}_2^-$  than APPJ. However, important differences were recorded among both sources with regard to generation of short-lived RONS: kINPen being much more effective than APPJ from short treatment times.

**CAP does not affect physic-chemical properties of alginate.** In this section 2 mL of 0.5% alginate were treated with either kINPen or APPJ under selected conditions (10 mm, 1 L/min) (pictures shown in Fig. 3c). The pH of plasma-treated alginate with any of both plasma jets remained unchanged with treatment time (Fig. 2b). This contrasts to the pH of Ringer's saline that decreased down to pH between 3.2 and 3.7 after 3 min of treatment.

Typical porous structures of lyophilized alginate (Fig. 3a) were observed by Scanning Electron Microscopy (SEM) and no differences were found after the plasma treatment. Similarly, Fourier Transform Infrared (FTIR-ATR) spectra of the 0.5% alginate (Fig. 3b) revealed no significant shifts between the different plasma jets studied (i.e., less than  $5 \text{ cm}^{-1}$ ). According to the literature, FTIR-ATR spectra of the sodium alginate presents seven characteristic bands from 2000 to  $650 \text{ cm}^{-1}$  region of the FTIR spectra<sup>15,16</sup> which remain unaltered with plasma treatment either using kINPen or plasma needle, indicating that plasma jet treatment of the solution did neither affect the main chemical bonds of the polymer network nor the ability of the solution to form a hydrogel (Fig. 3d). Only a minor change in intensity is found in the broad  $-\text{OH}$  stretching band within the  $3400\text{--}3200 \text{ cm}^{-1}$  range (not shown). This peak corresponds to a convolution envelope including both FTIR bands from water molecules (usually appearing between  $3700\text{--}3100 \text{ cm}^{-1}$ )<sup>17</sup> and the bands that correspond to the hydroxyl

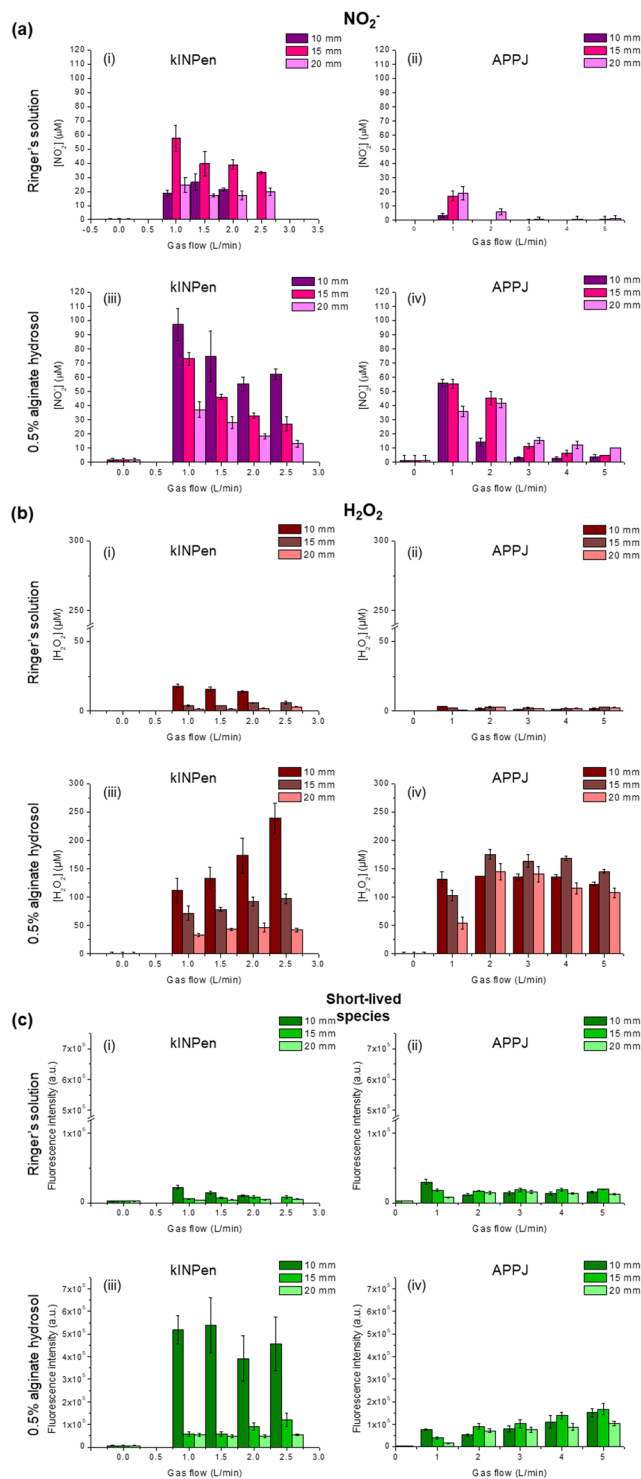


**Figure 1.** Influence of kINPen (left) or APPJ (right) distance to the sample and gas flow on the generation of  $\text{NO}_2^-$  (a),  $\text{H}_2\text{O}_2$  (b) and short-lived species (c) in Ringer's saline and in 0.5% alginate solutions. Treatment time was fixed at 90 s.

groups from the hydrogel. Since this peak can be highly dependent on the freeze-drying process of the samples, this hampers drawing conclusions from the peaks appearing in this range.

**Crosslinking is a critical step.** Since our final aim was to evaluate the ability of hydrogels to act as reservoirs for RONS generated by plasma, crosslinking of the alginate was an essential step. Thus, the 0.5% alginate solutions were plasma-treated, cross-linked for 5 min in a  $\text{CaCl}_2$  solution, and then rinsed to eliminate excess of crosslinker that could be toxic for further cell testing.

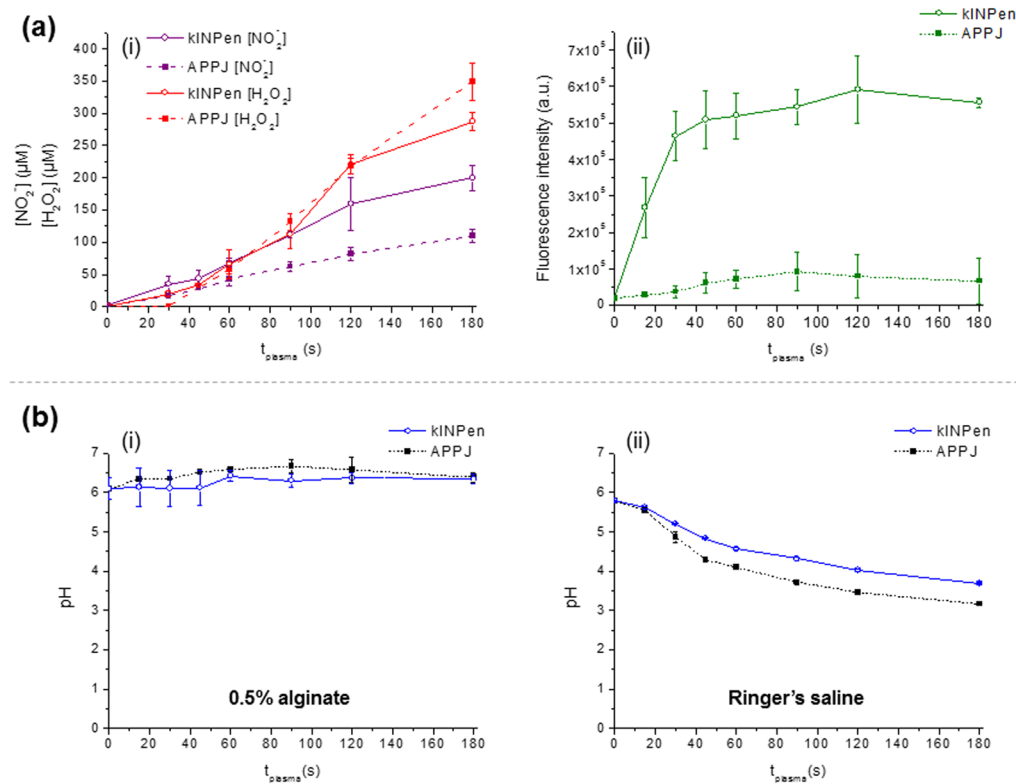


**Figure 2.** Influence of plasma treatment time on the generation of  $\text{NO}_2^-$ ,  $\text{H}_2\text{O}_2$  (i) and short-lived species (ii) in 0.5% alginate using kINPen or APPJ at 1 L/min and 10 mm distance (a). pH evolution as function of plasma treatment time of 0.5% alginate (i) and Ringer's saline (ii) (b).

A significant part of the RONS generated by plasma in the alginate was released during the crosslinking process (Fig. 4). Most  $\text{NO}_2^-$  was lost from plasma-treated alginate during its crosslinking (51.8% for kINPen and 66.7% for APPJ) and the rinsing process (14.8% and 25.8%, respectively). Thus, these steps left the alginate hydrogel with only 33.4% for kINPen and 7.5% for APPJ of the initial  $\text{NO}_2^-$  plasma-loading, which corresponds to 32.4  $\mu\text{M}$  and 25.2  $\mu\text{M}$  respectively.

In the case of  $\text{H}_2\text{O}_2$ , a lower fraction was lost during the whole crosslinking process (crosslinking + rinsing). A final percentage of 42.8% and 39.3% (in kINPen- and APPJ-treated alginate, respectively) remained in the hydrogel with respect to the initial loading, corresponding to final amounts of peroxides of 47.9  $\mu\text{M}$  and 115.8  $\mu\text{M}$ . These can be considered as the initial amount of nitrites and peroxides loaded in the alginate hydrogel at the beginning of the release experiments presented in Fig. 5.

**CAP-treated hydrogels are not cytotoxic.** The diffusion of species remaining in the plasma-treated alginate hydrogels after the crosslinking process to the cell culture medium (Fig. 5) was evaluated either in Transwell experiments or in direct contact with the medium.

Figures 5a,b show the respective  $\text{NO}_2^-$  and  $\text{H}_2\text{O}_2$  release kinetics from plasma-treated alginate hydrogel to the cell culture medium during 72 h, using the hydrogel in direct immersion (i) or using an insert (Transwell experiments) (ii). Direct immersion of the alginate hydrogel led to higher release amount of  $\text{NO}_2^-$  from the hydrogel than Transwell experiments. Plasma-treated hydrogel presented a maximum release of nitrites of  $30.01 \pm 8.05 \mu\text{M}$  for kINPen and  $22.68 \pm 2.77 \mu\text{M}$  for APPJ after 72 hours for direct immersion of the hydrogel, which corresponds to a 92.6% and 89.9% of the initial loading of  $\text{NO}_2^-$ .

Half  $\text{NO}_2^-$  release was recorded ( $14.65 \pm 3.29 \mu\text{M}$  and  $10.19 \pm 2.75 \mu\text{M}$ , respectively) when placing the hydrogel in an insert (this corresponds to 45.2% and a 40.4% of the initial concentration of nitrites in the hydrogel), in kINPen and in APPJ respectively.

Regarding  $\text{H}_2\text{O}_2$  release from the plasma-treated alginate (Fig. 5b), low amount of hydrogen peroxides was observed either in Transwell or in direct contact, with higher values of  $\text{H}_2\text{O}_2$  in the release media around 10  $\mu\text{M}$ .

The effect of the release of RONS from the plasma-treated alginate was studied on Sarcoma osteogenic cells (SaOS-2) and results are presented in Fig. 6. No significant differences were observed in SaOs-2 cell viability between untreated and plasma-treated crosslinked hydrogels placed in Transwell with respect to control, either for 24 or 72 hours. After crosslinking the hydrogels had undergone washing process, so few RONS remained in the material. Therefore, the lack of toxicity in the crosslinked hydrogels indicates that the plasma treatment of the alginate did not induce cytotoxic alterations in the alginate chains. In contrast, non-crosslinked alginate solutions presented a decrease of cell viability after 72 hours with respect to control, with cell viability of 76.0% for UT NC and 65.9% and 63.9% for APPJ180 NC and kINPen180 NC, respectively.

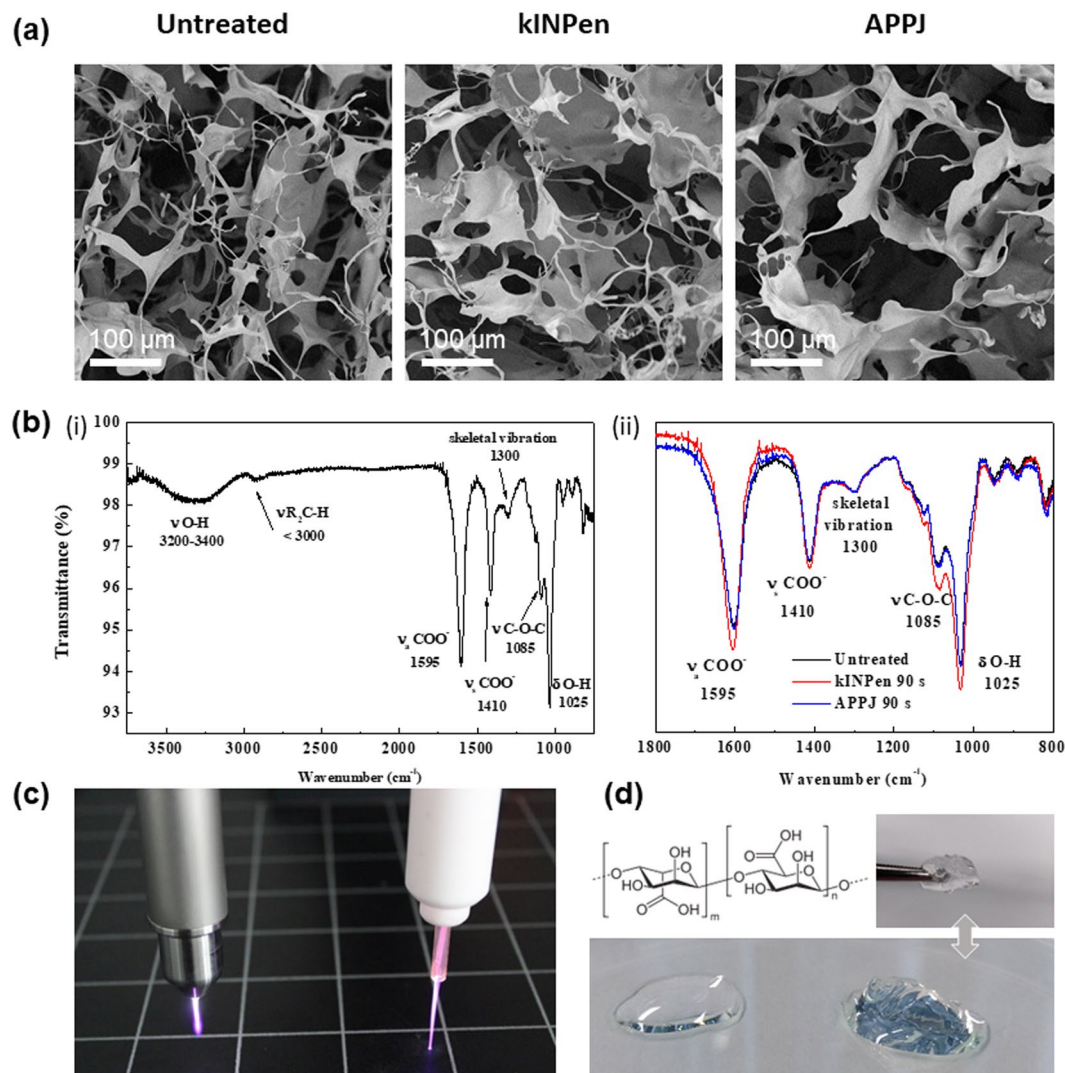


**Figure 3.** SEM micrographs (a) and FTIR-ATR spectra (b) of untreated (i), kINPen- and APPJ-treated 0.5% alginate for 90 s, at 10 mm distance and 1 L/min. Digital picture of kINPen and APPJ in operation (c). Chemical structure of alginate and digital pictures of the alginate solution (left side) and of the cross-linked alginate hydrogel (right side) (d).

## Discussion

In this work alginate hydrogels have been shown to be suitable vehicles for RONS produced by atmospheric pressure plasma jets. It is widely admitted that the CAP-generated RONS are basic anti-cancer factors suppressing cancer cell proliferation in *in vitro* cell cultures<sup>18–23</sup> and are also essential in the treatment of chronic wounds<sup>24</sup>. Here, two atmospheric pressure plasma jets are compared: a single-electrode jet working with helium and the kINPen, a widely extended plasma jet working with argon. The rationale for selecting these two jets with different characteristics is to allow for easier extrapolation of the results.

It is known that a variety of RONS can be formed by CAP in water or saline solutions such as Phosphate Buffer Saline (PBS)<sup>25–29</sup> and, as recorded here, in Ringer's saline. Many parameters affect the generation of RONS in solutions, the differences in chemical composition of the treated solution being critical to that aim<sup>6</sup>. Three species were quantified here:  $\text{H}_2\text{O}_2$ ,  $\text{NO}_2^-$  and long-lived species (Fig. 1(a–c) (i, ii)), their concentration increasing with treatment time (Fig. 2a) with both plasma jets, APPJ and kINPen. As reviewed by Jablonowski *et al.*<sup>24</sup>, RONS in the liquid phase can either be generated by direct interaction at the plasma/liquid interface<sup>21,30</sup>, via transfer of the reactive species from the gas phase into the liquid<sup>31,32</sup>, or by secondary or tertiary reactions in the bulk liquid<sup>2</sup>.

It can be observed that the concentration of RONS generated in alginate was several-fold higher than in Ringer's saline, ranging between 2 ( $\text{NO}_2^-$ ), 10 ( $\text{H}_2\text{O}_2$ ) and 25 (short-lived RONS) -fold higher for kINPen and slightly lower for the He APPJ needle. This can be explained by the following: Nitrites are formed in plasma treated liquids through the dissolution of nitrogen oxides formed in the gas phase of the plasma jet. In general, in acidic conditions, nitrous acid (which is one of the major sources of  $\text{NO}_2^-$ ) is not stable and decomposes into nitrogen dioxide, which may react with  $\text{OH}^\bullet$  to form peroxynitrous acid.

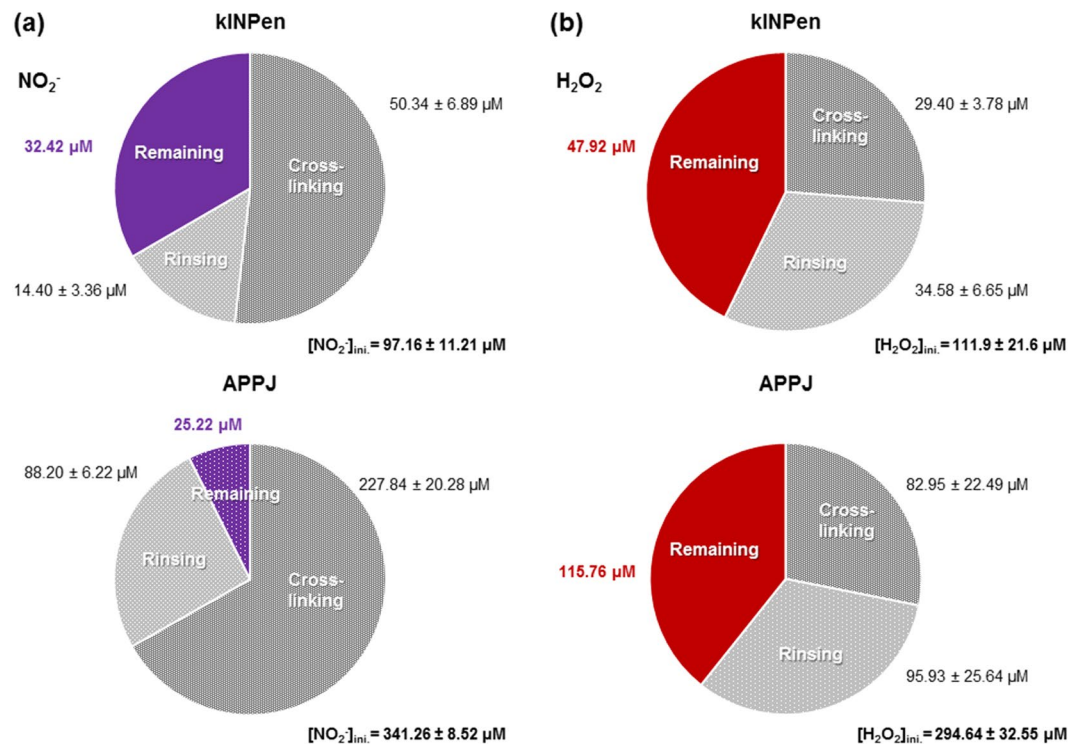
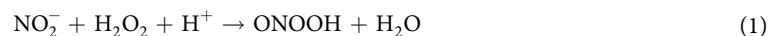


**Figure 4.** Total concentration of NO<sub>2</sub><sup>-</sup> (a) and H<sub>2</sub>O<sub>2</sub> (b) released during crosslinking and rinsing processes of the alginate hydrogel previously treated by kINPen for 90 s and APPJ for 15 min (10 mm, 1 L/min). The proportion of RONS remaining in the hydrogel after crosslinking and rinsing are highlighted in violet for NO<sub>2</sub><sup>-</sup> and red for H<sub>2</sub>O<sub>2</sub>.

Another reaction that is promoted in acidic solution takes place between NO<sub>2</sub><sup>-</sup> and H<sub>2</sub>O<sub>2</sub> (reaction 1) and is another source of peroxyxynitrites<sup>6,33–35</sup>.



Peroxyxynitrous acid is not stable at acidic pH and converts to NO<sub>3</sub><sup>-</sup>, as shown by Bruggeman *et al.*<sup>30</sup>.

As Ringer's saline is progressively acidified by the CAP treatment (Fig. 2b) - due to the formation of nitrites - these reactions can take place and decrease the amount of H<sub>2</sub>O<sub>2</sub> and NO<sub>2</sub><sup>-</sup> in the liquid (Fig. 1). On the contrary, the close to neutral pH found in the alginate solutions (Fig. 2b), avoids this reaction taking place and may allow for the accumulation of much higher concentrations of these RONS. This hypothesis is confirmed by CAP treatment of a buffered solution (PBS) at the same pH of 6.5 as alginate (Supplementary Fig. 2). It can be observed that the concentrations of RONS generated by CAP treatment in PBS are similar with those obtained in alginate.

The screening of the plasma treatment conditions pointed out that the amount of the different reactive species (NO<sub>2</sub><sup>-</sup>, H<sub>2</sub>O<sub>2</sub> and short-lived species) can be easily tuned, a crucial feature to be able to control the dose of RONS. For instance, as observed in other works<sup>36</sup>, on increasing the gas flow rate, after a certain point the concentration of NO<sub>2</sub><sup>-</sup> decreases for both plasma jets (Fig. 1a). This can possibly be ascribed to the fluid dynamics in the gas phase which play a major role in the species that can reach the liquid surface and thus, on the generation of RONS in liquids. It has been reported that at low flow rates the jet effluent follows a laminar mode that allows the mixing of air with the noble gas generating the discharge (and thus generation of more RONS in the gas phase)<sup>1,21,26,35</sup>. Contrarily, at higher gas flows, the effluent enters a turbulent mode that impairs mixing of air and decreases the amount of certain RONS generated<sup>21</sup>. For a deeper understanding of the reactions taking place in liquids, Verlackt *et al.*<sup>26</sup>, presented a 2D fluid dynamics model for the interaction between kINPen and a liquid (water). Despite the 0.5% alginate being more viscous than water, the plasma gas phase fluid dynamics may be extrapolated and the same descriptions valid at this point, since to our knowledge no modelling with hydrogels has been reported until now.

Alginate solutions are studied in this work given their ability to crosslink *in vivo* with Ca<sup>2+</sup> ions from the body and form stable hydrogels which can allow drug delivery of RONS with a minimally invasive strategy. The higher concentrations of RONS generated by CAP in alginate, which displayed no apparent changes in the structure of the polymer (Fig. 3) were progressively released to a surrounding medium (Fig. 5). However, to simulate the crosslinking in the laboratory and obtaining the hydrogel, it is necessary to add a CaCl<sub>2</sub> solution to the alginate solution. This leads to an important loss of the initial amount of RONS by diffusion to the crosslinking solution (Fig. 4). Although the loss of RONS in the crosslinking process could partly be limited during crosslinking by reducing the volume and increasing the concentration of CaCl<sub>2</sub> of the crosslinking solution, this leak of RONS is

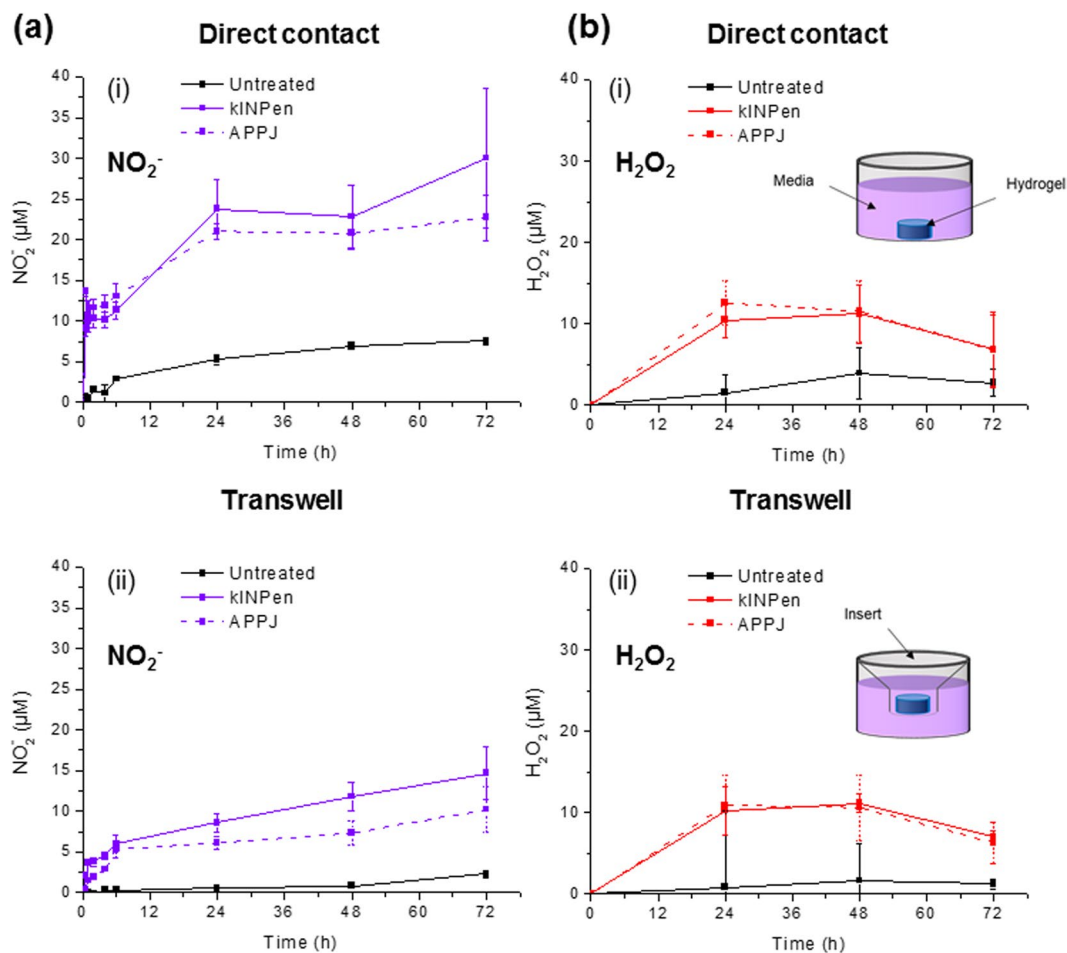


**Figure 5.** Cumulative release profiles of  $\text{NO}_2^-$  (a) and  $\text{H}_2\text{O}_2$  (b) from the RONS-loaded 0.5% alginate hydrogels to cell culture media. The alginate hydrogels had been treated by kINPen or APPJ for 90 s or 15 min, respectively (at 10 mm, 1 L/min), crosslinked and rinsed. Release was evaluated either in direct contact (i) or in Transwell (ii).

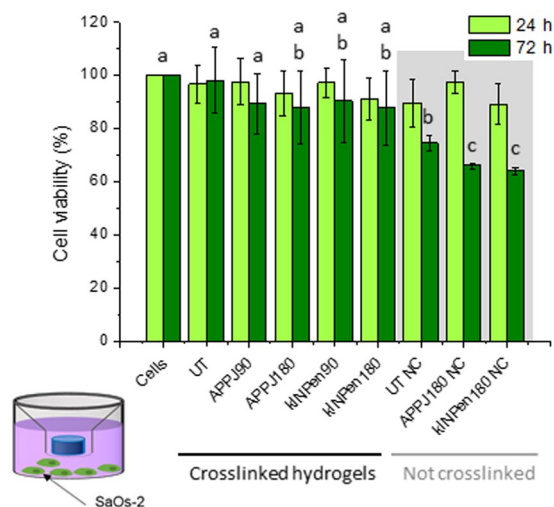


**Figure 6.** SaOS-2 cell viability of untreated (UT), APPJ- and kINPen-treated alginate hydrogels for 24- and 72-hour Transwell cell culture at treatment times of 90 and 180 s. Cell viability using non-crosslinked alginate solutions (NC) is presented on grey background. a,b,c indicate statistically significant differences.

inevitable if working *in vitro*. The final values of RONS in the final hydrogel are between 7% and 34% of the initial amounts generated by CAP in the alginate hydrosol, depending on the reactive species and the initial plasma treatment performed. In particular, the final amount remaining in the alginate hydrogel for further release of  $\text{NO}_2^-$  was  $32.4\ \mu\text{M}$  for 90 s kINPen treatment and  $25.2\ \mu\text{M}$  for 15 min APPJ treatment (10 mm, 1 L/min); concentration of  $\text{H}_2\text{O}_2$  was of  $47.9\ \mu\text{M}$  and  $115.8\ \mu\text{M}$ , respectively. These amounts of RONS are still higher in hydrogel compared to Ringer's saline (Fig. 1), which is an advantage to the use of alginate with respect to saline solution. Furthermore, for *in vivo* application, as crosslinking would take place in the body with the  $\text{Ca}^{2+}$  in body fluids, all RONS would be available for local delivery.

Release experiments showed final nitrite release of  $30.0\ \mu\text{M}$  for kINPen and  $22.7\ \mu\text{M}$  for APPJ-treated alginate hydrogel after 72 h, in direct contact with cell culture medium, corresponding to release percentages of 92.4% and 89.9% of the initial concentration, respectively. The final  $\text{NO}_2^-$  concentrations go down to  $14.7\ \mu\text{M}$  and  $10.2\ \mu\text{M}$ , respectively, when the plasma-treated hydrogels were placed in suspension in the cell culture media using an insert (same configuration between the release and cytotoxicity experiments). Regarding  $\text{H}_2\text{O}_2$ , the highest amount ( $\sim 10\ \mu\text{M}$ ) was obtained after 24 h of release for both plasma devices. A decreasing trend of  $\text{H}_2\text{O}_2$  concentration was observed in the release media from 48 to 72 hours, that may be attributed to an ageing of  $\text{H}_2\text{O}_2$ , as observed in cell culture media<sup>37</sup>.

The viability of SaOS-2 was not affected when cells were cultured in indirect contact with untreated and plasma-treated crosslinked hydrogels for both kinds of plasma treatments (Fig. 6). Despite the high loading of RONS in the alginate solutions achieved by plasma treatment, the low amount of RONS remaining after crosslinking (Figs 4 and 5) does not affect cell viability, which agrees with previous works<sup>6,38</sup>. As most RONS were washed away by the crosslinking + washing process, this allowed to ascertain that the biomaterial itself remains fully biocompatible after the plasma treatment (no significant differences were observed in crosslinked alginate between treatments or with respect to controls, Fig. 6).

To evaluate the biological efficacy of the plasma-generated RONS within the alginate, non crosslinked (NC) polymer solutions were employed (Fig. 6). A slight decrease in cell viability was observed for the untreated alginate solution (UT NC) that could be attributed to calcium sequestration from the cell culture media by the alginate. The plasma-generated RONS lead to a further decrease of cell viability from the untreated (UT NC) to the plasma-treated alginate solutions. Cell viability after 72 hours decreased to 65.9% for APPJ180 NC and 63.9% for kINPen180 NC, respectively. This decrease on SaOS-2 cell viability can be ascribed to the concentration of  $\text{H}_2\text{O}_2$  released to the media from the plasma-treated alginate solutions, and available for interaction with cells was of  $39.79 \pm 3.49\ \mu\text{M}$  for APPJ180 NC and  $37.68 \pm 2.96\ \mu\text{M}$  for kINPen180 NC.

The decrease in cell viability obtained with these levels of RONS is in line with previous works<sup>38</sup>, where APPJ plasma treatment of cell culture medium resulted in a progressive decrease of the viability of SaOS-2 with the increase of RONS concentration in culture media. In that work, cell viability was found between 92 and 20% for APPJ treatment times of 10–30 min. The higher cytotoxicity in that work<sup>38</sup> has to be directly related with the higher amount of RONS present in the McCoy's cell culture medium (ie.  $\text{H}_2\text{O}_2$ :  $98\ \mu\text{M}$  for 10 min APPJ treatment to  $290\ \mu\text{M}$  for 30 min APPJ treatment) with respect to the amounts found here. Despite here only  $\text{NO}_2^-$ ,  $\text{H}_2\text{O}_2$  and short-lived ROS were detected, many studies have described the anti-carcinogenic effects of plasma by many other reactive species such as  $\text{O}_2^-$ ,  $\text{OH}^\bullet$ ,  $\text{NO}$ ,  $\text{O}$ ,  $\text{NO}_3^-$ ,  $\text{NO}_2^-$  and  $\text{ONOO}^-$ <sup>21</sup>, and other works<sup>25,39</sup> investigated artificially supplementing liquids with the same concentrations of  $\text{H}_2\text{O}_2$  and/or  $\text{NO}_2^-$  and did not observe the same effects as with plasma, confirming the hypothesis that the complex of RONS generated by plasma is necessary for its biological action.

Thus, generating reactive species by cold atmospheric plasmas in alginate-based biomaterials and their release opens great perspectives in the design of new implantable biomaterials for plasma therapies. These results have important implications in many biomedical applications of alginate hydrogels, including tissue engineering and drug delivery.

## Methods

**Materials.** Sodium alginate (Na-alginate MW: 10000–600000 g/mol) in powder form was purchased from Panreac. Potassium chloride (KCl, Panreac), sodium chloride (NaCl, Sigma-Aldrich) and calcium chloride dehydrate ( $\text{CaCl}_2 \cdot 2\text{H}_2\text{O}$ , Sigma-Aldrich) were used for the preparation of Ringer's saline solution. Phosphoric acid (85%; MW: 98 g/mol, Panreac), sulphanilamide (M.W: 172.20 g/mol, Sigma-Aldrich) and N-(1-naphthyl)ethylenediamine (NEED, MW: 172.20 g/mol, Sigma-Aldrich) were used for synthesis of Griess reagent. Calcium chloride ( $\text{CaCl}_2$ , 96% anhydrous, MW: 110, 98 g/mol), sodium nitrite ( $\text{NaNO}_2$ , MW: 69 g/mol) and sodium azide ( $\text{NaN}_3$ , MW: 65 g/mol), in powder form, were obtained from Sigma-Aldrich. Titanyl oxysulphate ( $\text{TiOSO}_4$ , MW: 159.90 g/mol; 27–31%<sub>wt</sub> in  $\text{H}_2\text{SO}_4$ ), hydrogen peroxide ( $\text{H}_2\text{O}_2$ , MW: 34.01 g/mol; 30%<sub>wt/wt</sub> in  $\text{H}_2\text{O}$ ), peroxidase from Horseradish type VI (HRP) (250 U/mg, Sigma-Aldrich) and 2',7'-Dichlorofluorescein diacetate (DCFH-DA) ( $\geq 97\%$ ) were purchased from Sigma-Aldrich. Amplex Red reagent was provided by Invitrogen (ref. A12222). Helium and argon gas were provided by Praxair, Spain.

Sarcoma osteogenic cells (SaOs-2, ATCC, USA) were expanded in McCoy's 5A culture medium (Sigma Aldrich). Foetal Bovine Serum (FBS) and Penicillin/Streptomycin (P/S) (50 U/ml and  $50\ \mu\text{g/ml}$ , respectively) were purchased from Invitrogen. Cells from passage between 24 and 32 were used in all experiments. Cell Proliferation Reagent WST-1 used for cell viability determination was purchased from Roche Diagnostics GmbH (ref. 05015944001).

**Preparation of alginate solutions and hydrogels.** The alginate solutions were obtained by mixing the dry sodium-alginate powder with DI water in a SpeedMixer (DAC 150.1 FVZ-k, 3500 rpm) for 15 min at 0.5% w/w. Alginate solutions (or hydrosols), that refer to the physical state of the alginate before crosslinking of the polymer chains<sup>40</sup>, were stored at 4 C and used within a lifespan of 2 weeks. The alginate hydrogels were obtained

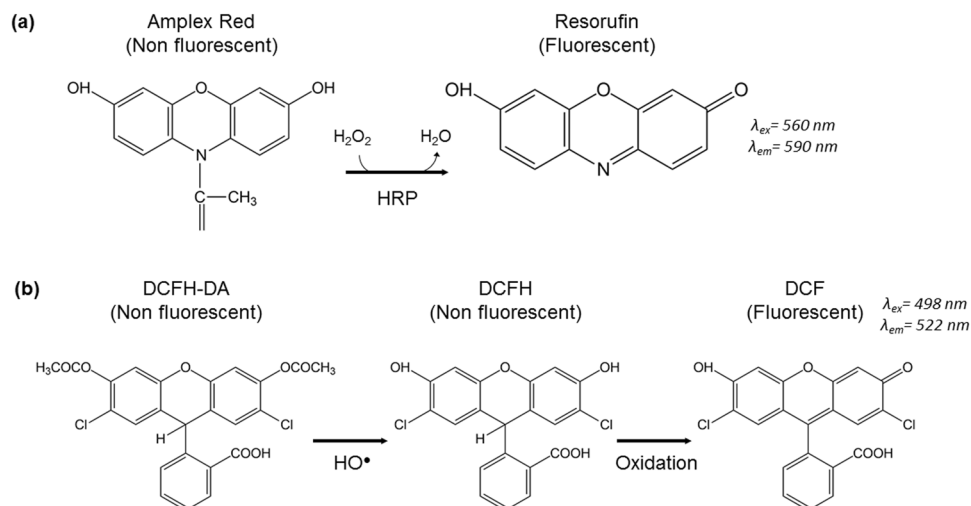


**Figure 7.** Chemical reactions involved in the fluorescent probes used for the detection of  $\text{H}_2\text{O}_2$  (a) and short-lived reactive species (b) in alginate hydrosol.

by ionic crosslinking of the hydrosol using a 150  $\mu\text{L}$  of a 50 mM calcium chloride ( $\text{CaCl}_2$ ) solution for 200  $\mu\text{L}$  of alginate hydrosol for 5 min. Subsequent rinsing using 100  $\mu\text{L}$  of DI water of the formed hydrogel was performed for 5 minutes before its use for release and cell culture experiments, to eliminate the excess of calcium coming from the crosslinking solution. Crosslinking and rinsing solution used for obtaining the hydrogel were kept for determination of  $[\text{NO}_2^-]$  and  $[\text{H}_2\text{O}_2]$ , and the formed hydrogels were used for 72-hour release experiments. For cell experiments using alginate hydrogels, all the processes leading to the preparation of the formed hydrogel were carried out under sterile conditions. Alginate powder was sterilized by low-pressure plasma treatment using a low-pressure radio-frequency plasma.

**Plasma treatments.** In this study, two kinds of atmospheric plasma jet were used: a commercially available cold atmospheric plasma jet kINPen IND (NEOPLAS Tools, Germany)<sup>6</sup>, operating with argon and an atmospheric pressure plasma jet (APPJ) using He as plasma gas in a jet design based on a single electrode as described elsewhere<sup>41</sup> (Fig. 3c). Gas flow was regulated between 1 and 2.5 L/min for kINPen and between 1 and 5 L/min for APPJ by using Ar and He Bronkhorst Mass View flow controllers (BRONKHORST, Netherlands), respectively.

All plasma treatments of alginate for RONS quantification were performed on 200  $\mu\text{L}$  of the alginate solution (before crosslinking) in 96-well plates, with a distance between the nozzle and the sample surface between 10 and 20 mm.

**Detection of RONS in alginate hydrosols.** Determination of  $\text{NO}_2^-$  concentration in plasma-treated alginate hydrosol was performed using Griess reagent<sup>30,35,42,43</sup>. The Griess reagent used was obtained by dissolving 1%<sub>w/v</sub> of sulphanilamide, 0.1%<sub>w/v</sub> of NEEDED and 5%<sub>w/v</sub> of phosphoric acid in de-ionized water. 200  $\mu\text{L}$  of Griess reagent were added on 200  $\mu\text{L}$  of sample in 96 well-plates. The plates were incubated for 10 min at room temperature protected from the light. The absorbance was measured at  $\lambda_{\text{abs}} = 540 \text{ nm}$  using a Synergy HTX Hybrid Multi Mode Microplate Reader (BioTek Instruments, Inc., USA). The  $[\text{NO}_2^-]$  in each sample was determined from the absorbance values by using a calibration curve made from  $\text{NaNO}_2$  dilutions in alginate hydrosols.

The concentration of hydrogen peroxide was determined by reaction of  $\text{H}_2\text{O}_2$  with Amplex Red in presence of HRP enzyme that leads to the creation of resorufin, a fluorescent product (Fig. 7a). Amplex Red/HRP reagent consists in 100  $\mu\text{M}$  of Amplex Red and 0.25 U/mL HRP in DI water. Since the higher concentration of  $\text{H}_2\text{O}_2$  able to be processed properly by this reagent is around 10  $\mu\text{M}$  of  $\text{H}_2\text{O}_2$ , plasma-treated alginate hydrosols were diluted 200 times previously to the addition of the reagent. In this case, for hydrogen peroxide detection, 50  $\mu\text{L}$  of the Amplex Red/HRP reagent was added to 200  $\mu\text{L}$  of the 200 $\times$ -diluted alginate sample in a 96-well plate and incubated for 30 min at 37  $^\circ\text{C}$ . Subsequent fluorescence measurements were performed by means of a Synergy HTX Hybrid Multi Mode Microplate Reader (BioTek Instruments, Inc., USA), with fluorescence filters centred at  $\lambda_{\text{ex}} = 560/20 \text{ nm}$  and  $\lambda_{\text{em}} = 590/20 \text{ nm}$  as excitation and emission wavelengths, respectively. Concentrations of  $\text{H}_2\text{O}_2$  in alginate hydrosol generated by plasma treatment were obtained from the fluorescence values using a calibration curve made from 30% hydrogen peroxide solution in alginate.

Presence of short-lived RONS was determined *in situ* in plasma-treated 0.5% alginate solution using 2',7'-Dichlorodihydrofluorescein diacetate (DCFH-DA), which is a scavenger of short-lived RONS<sup>44</sup>. DCFH-DA is a non-fluorescent dye which is hydrolyzed into its polar, but non-fluorescent form DCFH on the action of  $\text{HO}^\bullet$  radicals. Oxidation of DCFH by the action of reactive oxygen species (ROS) turns the molecule into its highly fluorescent form 2,7-Dichlorofluorescein (DCF) that can be detected by fluorescence<sup>42</sup> (Fig. 7b). Since 2',7'-DCFH is a non-specific probe and can react with various short-lived species, such as  $\text{OH}^\bullet$ ,  $\text{HOO}^\bullet$ ,  $\text{NO}^\bullet$ ,  $\text{H}_2\text{O}_2$ ,  $\text{ONOO}^\bullet$ <sup>35,45,46</sup>, and due to the short lifespan of these species, no calibration curve can be done and results are expressed in fluorescence intensity. DCFH was previously incorporated to alginate hydrosol before plasma treatments in proportion 1  $\mu\text{L}$  of 2 mM 2,7-DCHF for 150  $\mu\text{L}$  of alginate hydrosol. 200  $\mu\text{L}$  of the alginate sample

containing DCHF were placed in 96-well black plate for plasma treatment. After 30-min incubation at room temperature, fluorescence intensity was read with a Synergy HTX Hybrid Multi Mode Microplate Reader using  $\lambda_{\text{ex}} = 485/20 \text{ nm}$  and  $\lambda_{\text{em}} = 528/20 \text{ nm}$  as excitation and emission wavelength filters, respectively.

As control, 0.9% Ringer's solution was used, performed in the same treatment conditions as alginate hydrosol. Ringer's saline was prepared by dissolving 8.60 g/L NaCl, 0.30 g/L KCl and 0.33 g/L  $\text{CaCl}_2 \cdot 2\text{H}_2\text{O}$  in DI water, filtered by using 0.22- $\mu\text{m}$  pore size MILLEXGP filter unit (Merck Millipore Ltd., Ireland).

**pH monitoring.** 2 mL of 0.5% alginate were placed in a 24 well-plates and treated using kINPen and APPJ (10 mm, 1 L/min). pH was measured by using a PC80 Multiparameter instrument (XS Instruments, Italy) with a Crison 50 14 electrode (Crison, Spain).

**FTIR-ATR.** FTIR-ATR spectra of freeze-dried alginate hydrogels were recorded using a Nicolet 6700 spectrometer (Thermo Scientific), equipped with a Universal ATR sampling device with a germanium crystal. Spectra were acquired at room temperature in transmission mode as a function of the  $\lambda$  ranged between 4 000 and 675  $\text{cm}^{-1}$  with 64 scans at a resolution of 1  $\text{cm}^{-1}$ . A background spectrum of air was scanned under the same instrumental conditions before each series of measurements.

**SEM.** Lyophilized 0.5% alginate hydrosols were C-coated using an EMITECH K950X Turbo Evaporator (Quorum Technologies Ltd., UK). All samples were imaged in a Phenom XL SEM (Phenom-World B.V., The Netherlands) under high vacuum at 5 kV and a 5 mm working distance.

**Release of RONS.** 200  $\mu\text{L}$  of 0.5% alginate hydrosol in 96-well plate were treated by kINPen for 90 s, 10 mm and 1 L/min and APPJ for 15 min, 10 mm and 1 L/min. Since lower amount of  $\text{NO}_2^-$  are generated in alginate with APPJ than kINPen, a longer plasma treatment time for APPJ has been performed to be able to reasonably detect  $[\text{NO}_2^-]$  with absorbance values within the plate-reader working range. 200  $\mu\text{L}$  of untreated and plasma-treated hydrogels were cross-linked in a 96-well plate by using 50 mM  $\text{CaCl}_2$  solution for 5 min. Afterward, formed alginate hydrogels were transferred to another well with 100  $\mu\text{L}$  distilled water for rinsing of the excess of calcium chloride solution for 5 min. Plasma treatments and crosslinking process for RONS release experiments were carried out in the same conditions used for cell culture experiments to be able to relate the release of RONS from the alginate hydrosol with the biological effects.

Formed alginate hydrogels were transferred to CORNING Transwell polyester membrane cell culture insert (Sigma-Aldrich), with a 6.5 mm diameter and a 0.4  $\mu\text{m}$  pore size and placed in suspension in 1 mL volume of cell culture media in 24-well plates. For the monitoring of the release kinetics of RONS from the alginate hydrogels 100  $\mu\text{L}$  of the cell culture medium used as release media were withdrawn at determined time points for subsequent quantification of  $\text{NO}_2^-$  and  $\text{H}_2\text{O}_2$ . 100  $\mu\text{L}$  of fresh medium was replaced after each sample collection. Final volumes of release media have been measured at the end of release experiment to take into account the volume correction in the concentration calculations of  $\text{NO}_2^-$  and  $\text{H}_2\text{O}_2$ .  $\text{NO}_2^-$  and  $\text{H}_2\text{O}_2$  were quantified as described in the previous section.

**In vitro cell experiments.** *Cell culture.* Sarcoma Osteogenic (SaOs-2) were used to study the cytotoxicity of the alginate hydrogels. The cell culture medium consisted of McCoy's 5A with 10% FBS and 1% P/S. Cells were grown in 75  $\text{cm}^2$  cell culture flasks at 37 °C in a 5%  $\text{CO}_2$  incubator and upon reaching 80% confluence. SaOs-2 were detached from the flask using trypsin (Invitrogen, ThermoFisher) and 10000 cells/well were seeded into 24-well plates with 1 mL volume of culture medium. After 6 h-adhesion, plasma-treated sterile alginate hydrogels, previously prepared in sterile conditions, were introduced into a CORNING Transwell polyester membrane cell culture insert and placed in suspension in the well, to evaluate the effect of kINPen and APPJ plasma treatment of the alginate hydrogels on the SaOs-2 cell viability. As positive control, the same number of cells was placed without adding alginate. The cells were grown at 37 °C in a 5%  $\text{CO}_2$  incubator for another 72 h.

*Cell viability.* Influence of plasma-treated 0.5% alginate hydrogels on SaOs-2 cell viability was evaluated for kINPen and APPJ (10 mm, 1 L/min) for 90 and 180 s of plasma treatments. Plasma-treated alginate solutions were also studied for 180 s APPJ and kINPen plasma treatment. Cell viability was evaluated at 0, 24 and 72 hours. Cell culture media was replaced by preparation consisting of 250  $\mu\text{L}$  of Cell Proliferation Reagent WST-1 in McCoy's culture medium (1:10) and incubated for 1 hour at 37 °C. Afterward, 100  $\mu\text{L}$  of the supernatant were transferred to another well for absorbance measurement at 440 nm. To evaluate the effects untreated and plasma-treated alginate hydrogels on SaOs-2 cell viability, normalization of the values was made with respect to the well containing cells only.

Received: 26 March 2019; Accepted: 21 October 2019;

Published online: 06 November 2019

## References

1. Reuter, S., von Woedtke, T. & Weltmann, K.-D. The kINPen—a review on physics and chemistry of the atmospheric pressure plasma jet and its applications. *J. Phys. D: Appl. Phys.* **51**, 233001 (2018).
2. Hoffmann, C., Berganza, C. & Zhang, J. Cold Atmospheric Plasma: methods of production and application in dentistry and oncology. *Med. Gas Res.* **3**, 21 (2013).
3. Dubuc, A. *et al.* Use of cold-atmospheric plasma in oncology: a concise systematic review. *Ther. Adv. Med. Oncol.* **10**, 1758835918786475 (2018).
4. Hartwig, S. *et al.* Treatment of Wound Healing Disorders of Radial Forearm Free Flap Donor Sites Using Cold Atmospheric Plasma: A Proof of Concept. *J. Oral Maxillofac. Surg.* **75**, 429–435 (2017).

5. Rutkowski, R., Pancewicz, S. A., Rutkowski, K. & Rutkowska, J. Reactive oxygen and nitrogen species in inflammatory process. *Pol. Merkur. Lekarski* **23**, 131–136 (2007).
6. Khluyustova, A., Labay, C., Machala, Z., Ginebra, M.-P. & Canal, C. Important parameters in plasma jets for the production of RONS in liquids for plasma medicine: a brief review. *Front. Chem. Sci. Eng.* **13**, 238–252 (2019).
7. Shen, J. *et al.* Bactericidal Effects against *S. aureus* and Physicochemical Properties of Plasma Activated Water stored at different temperatures. *Sci. Rep.* **6**, 28505 (2016).
8. Drury, J. L. & Mooney, D. J. Hydrogels for tissue engineering: Scaffold design variables and applications. *Biomaterials* **24**, 4337–4351 (2003).
9. Tan, H. & Marra, K. G. Injectable, Biodegradable Hydrogels for Tissue Engineering Applications. *Materials (Basel)*. **3**, 1746–1767 (2010).
10. Omidian, H. & Park, K. Hydrogels. In *Fundamentals and Applications of Controlled Release Drug Delivery* 75–105, [https://doi.org/10.1007/978-1-4614-0881-9\\_4](https://doi.org/10.1007/978-1-4614-0881-9_4) (Springer US, 2012).
11. Nguyen, M. K. & Lee, D. S. Injectable Biodegradable Hydrogels. *Macromol. Biosci.* **10**, 563–579 (2010).
12. Rowley, J. A., Madlambayan, G. & Mooney, D. J. Alginate hydrogels as synthetic extracellular matrix materials. *Biomaterials* **20**, 45–53 (1999).
13. Mørch, Y. A., Donati, I. & Strand, B. L. Effect of Ca<sup>2+</sup>, Ba<sup>2+</sup>, and Sr<sup>2+</sup> on Alginate Microbeads. *Biomacromolecules* **7**, 1471–1480 (2006).
14. Lee, K. Y. & Mooney, D. J. Alginate: properties and biomedical applications. *Prog. Polym. Sci.* **37**, 106–126 (2012).
15. Daemi, H. & Barikani, M. Synthesis and characterization of calcium alginate nanoparticles, sodium homopolymannuronate salt and its calcium nanoparticles. *Sci. Iran.* **19**, 2023–2028 (2012).
16. Li, P., Dai, Y.-N., Zhang, J.-P., Wang, A.-Q. & Wei, Q. Chitosan-Alginate Nanoparticles as a Novel Drug Delivery System for Nifedipine. *Int. J. Biomed. Sci.* **4**, 221–228 (2008).
17. Enev, V., Sedláček, P., Jarábková, S., Velcer, T. & Peřkař, M. ATR-FTIR spectroscopy and thermogravimetry characterization of water in polyelectrolyte-surfactant hydrogels. *Colloids Surf. A* **575**, 1–9 (2019).
18. Yan, D. *et al.* The Strong Cell-based Hydrogen Peroxide Generation Triggered by Cold Atmospheric Plasma. *Sci. Rep.* **7**, 10831 (2017).
19. Yan, D. *et al.* Toward understanding the selective anticancer capacity of cold atmospheric plasma—A model based on aquaporins (Review). *Biointerphases* **10**, 40801 (2015).
20. Yan, D., Sherman, J. H. & Keidar, M. Cold atmospheric plasma, a novel promising anti-cancer treatment modality. *Oncotarget* **28**, 15977–15995, <https://doi.org/10.18632/oncotarget.13304> (2017).
21. Lu, X. *et al.* Reactive species in non-equilibrium atmospheric-pressure plasmas: Generation, transport, and biological effects. *Phys. Rep.* **630**, 1–84 (2016).
22. Hirst, A. M., Frame, F. M., Arya, M., Maitland, N. J. & O’Connell, D. Low temperature plasmas as emerging cancer therapeutics: the state of play and thoughts for the future. *Tumor Biol.* **37**, 7021–7031 (2016).
23. Keidar, M. Plasma for cancer treatment. *Plasma Sources Sci. Technol.* **24**, 33001 (2015).
24. Jablonowski, H., Santos Sousa, J., Weltmann, K.-D., Wende, K. & Reuter, S. Quantification of the ozone and singlet delta oxygen produced in gas and liquid phases by a non-thermal atmospheric plasma with relevance for medical treatment. *Sci. Rep.* **8**, 12195 (2018).
25. Van Boxem, W. *et al.* Anti-cancer capacity of plasma-treated PBS: Effect of chemical composition on cancer cell cytotoxicity. *Sci. Rep.* **7**, 16478, <https://doi.org/10.1038/s41598-017-16758-8> (2017).
26. Verlackt, C. C. W., Van Boxem, W. & Bogaerts, A. Transport and accumulation of plasma generated species in aqueous solution. *Phys. Chem. Chem. Phys.* **20**, 6845–6859 (2018).
27. Tanaka, H. *et al.* Non-thermal atmospheric pressure plasma activates lactate in Ringer’s solution for anti-tumor effects. *Sci. Rep.* **6**, 36282 (2016).
28. Gorbanev, Y., Privat-Maldonado, A. & Bogaerts, A. Analysis of Short-Lived Reactive Species in Plasma-Air-Water Systems: The Dos and the Do Nots. *Anal. Chem.* **90**, 13151–13158 (2018).
29. Chauvin, J., Judée, F., Yousfi, M., Vicendo, P. & Merbahi, N. Analysis of reactive oxygen and nitrogen species generated in three liquid media by low temperature helium plasma jet. *Sci. Rep.* **7**, 4562 (2017).
30. Bruggeman, P. J. *et al.* Plasma-liquid interactions: A review and roadmap. *Plasma Sources Science and Technology* **25**, 053002, <https://doi.org/10.1088/0963-0252/25/5/053002> (2016).
31. Attri, P. *et al.* Generation mechanism of hydroxyl radical species and its lifetime prediction during the plasma-initiated ultraviolet (UV) photolysis. *Sci. Rep.* **5**, 9332 (2015).
32. Winter, J. *et al.* Tracking plasma generated H<sub>2</sub>O<sub>2</sub> from gas into liquid phase and revealing its dominant impact on human skin cells. *J. Phys. D: Appl. Phys.* **47**, <https://doi.org/10.1088/0022-3727/47/28/285401> (2014).
33. Bosi, F. J. *et al.* Characterization and comparative evaluation of two atmospheric plasma sources for water treatment. *Plasma Process Polym.* **15**, e1700130 (2018).
34. Clupek, P. L. *et al.* Aqueous-phase chemistry and bactericidal effects from an air discharge plasma in contact with water: evidence for the formation of peroxyxynitrite through a pseudo-second-order post-discharge reaction of H<sub>2</sub>O<sub>2</sub> and HNO<sub>2</sub>. *Plasma Sources Sci. Technol.* **23**, 15019 (2014).
35. Machala, Z. *et al.* Formation of ROS and RNS in water electro-sprayed through transient spark discharge in air and their bactericidal effects. *Plasma Process. Polym.* **10**, 649–659 (2013).
36. Baek, E. *et al.* Effects of the electrical parameters and gas flow rate on the generation of reactive species in liquids exposed to atmospheric pressure plasma jets. *Physics of Plasmas* **23**, 073515 (2016).
37. Yan, D. *et al.* Stabilizing the cold plasma-stimulated medium by regulating medium’s composition. *Sci. Rep.* **6**, 26016 (2016).
38. Canal, C. *et al.* Plasma-induced selectivity in bone cancer cells death. *Free Radic. Biol. Med.* **110**, 72–80 (2017).
39. Tornin, J. *et al.* Pyruvate plays a main role in the antitumoral selectivity of cold atmospheric plasma in osteosarcoma. *Sci. Rep.* **9**(1), 10681 (2019).
40. Omidian, H. & Park, K. *Introduction to Hydrogels BT - Biomedical Applications of Hydrogels Handbook*. In (eds Ottenbrite, R. M., Park, K. & Okano, T.) 1–16, [https://doi.org/10.1007/978-1-4419-5919-5\\_1](https://doi.org/10.1007/978-1-4419-5919-5_1) (Springer New York, 2010).
41. Zaplotnik, R. *et al.* Influence of a sample surface on single electrode atmospheric plasma jet parameters. *Spectrochim. Acta Part B At. Spectrosc.* **103–104**, 124–130 (2015).
42. Guevara, I. *et al.* Determination of nitrite/nitrate in human biological material by the simple Griess reaction. *Clin. Chim. Acta.* **274**, 177–188 (1998).
43. Giustarini, D., Rossi, R., Milzani, A. & Dalle-Donne, I. Nitrite and nitrate measurement by Griess reagent in human plasma: evaluation of interferences and standardization. *Methods Enzymol.* **440**, 361–380 (2008).
44. Gomes, A., Fernandes, E. & Lima, J. L. F. C. Fluorescence probes used for detection of reactive oxygen species. *J. Biochem. Biophys. Methods* **65**, 45–80 (2005).
45. Rajneesh, J., Pathak, J., Chatterjee, A., Singh, S. P. & Sinha, R. P. Detection of Reactive Oxygen Species (ROS) in Cyanobacteria Using the Oxidant-sensing Probe 2',7'-Dichlorodihydrofluorescein Diacetate (DCFH-DA). *Bio-protocol* **7**, e2545 (2017).
46. Rastogi, R. P., Singh, S. P., Häder, D.-P. & Sinha, R. P. Detection of reactive oxygen species (ROS) by the oxidant-sensing probe 2',7'-dichlorodihydrofluorescein diacetate in the cyanobacterium *Anabaena variabilis* PCC 7937. *Biochem. Biophys. Res. Commun.* **397**, 603–607 (2010).

## Acknowledgements

This project has received funding from the European Research Council (ERC) under the European Union's Horizon 2020 research and innovation programme (grant agreement No. 714793). Authors acknowledge the financial support of MINECO for MAT2015-65601-R project (MINECO/FEDER, EU) and for the RyC fellowship of C.C.; and of Generalitat de Catalunya for the 2017SGR-1165 project and the ICREA Academia Award for excellence in research of M.P.G.

## Author contributions

Cédric Labay contributed to the experimental design and performed most of the experimental work (RONS detection, release experiments and *in vitro* assays). He was involved in the acquisition, analysis and interpretation of data. He contributed to the writing and revision of the manuscript. Inès Hamouda participated to the experimental work related with sample preparation, RONS detection and FTIR-ATR data acquisition. She also took part in the revision of the manuscript. Francesco Tampieri contributed to the revision of the paper, the complementary experiments performed during the revision and worked on the interpretation of the new results and discussion. Maria-Pau Ginebra contributed substantively to the experimental design, the interpretation of data and the revision of the manuscript. Cristina Canal contributed to the conception of the work, the experimental design, the analysis and interpretation of data as well as to the writing and the revision of the manuscript. All authors have approved the submitted version; All authors have agreed both to be personally accountable for the author's own contributions and to ensure that questions related to the accuracy or integrity of any part of the work, even ones in which the author was not personally involved, are appropriately investigated, resolved, and the resolution documented in the literature.

## Competing interests

The authors declare no competing interests.

## Additional information

**Supplementary information** is available for this paper at <https://doi.org/10.1038/s41598-019-52673-w>.

**Correspondence** and requests for materials should be addressed to C.C.

**Reprints and permissions information** is available at [www.nature.com/reprints](http://www.nature.com/reprints).

**Publisher's note** Springer Nature remains neutral with regard to jurisdictional claims in published maps and institutional affiliations.



**Open Access** This article is licensed under a Creative Commons Attribution 4.0 International License, which permits use, sharing, adaptation, distribution and reproduction in any medium or format, as long as you give appropriate credit to the original author(s) and the source, provide a link to the Creative Commons license, and indicate if changes were made. The images or other third party material in this article are included in the article's Creative Commons license, unless indicated otherwise in a credit line to the material. If material is not included in the article's Creative Commons license and your intended use is not permitted by statutory regulation or exceeds the permitted use, you will need to obtain permission directly from the copyright holder. To view a copy of this license, visit <http://creativecommons.org/licenses/by/4.0/>.

© The Author(s) 2019